# Compressive Sensing-Based Detection with Multimodal Dependent Data

Thakshila Wimalajeewa *Member IEEE*, and Pramod K. Varshney, *Fellow IEEE*

*Abstract*—Detection with high dimensional multimodal data is a challenging problem when there are complex inter- and intra- modal dependencies. While several approaches have been proposed for dependent data fusion (e.g., based on copula theory), their advantages come at a high price in terms of computational complexity. In this paper, we treat the detection problem with compressive sensing (CS) where compression at each sensor is achieved via low dimensional random projections. CS has recently been exploited to solve detection problems under various assumptions on the signals of interest, however, its potential for dependent data fusion has not been explored adequately. We exploit the capability of CS to capture statistical properties of uncompressed data in order to compute decision statistics for detection in the compressed domain. First, a Gaussian approximation is employed to perform likelihood ratio (LR) based detection with compressed data. In this approach, inter-modal dependence is captured via a compressed version of the covariance matrix of the concatenated (temporally and spatially) uncompressed data vector. We show that, under certain conditions, this approach with a small number of compressed measurements per node leads to enhanced performance compared to detection with uncompressed data using widely considered suboptimal approaches. Second, we develop a nonparametric approach where a decision statistic based on the second order statistics of uncompressed data is computed in the compressed domain. The second approach is promising over other related nonparametric approaches and the first approach when multimodal data is highly correlated at the expense of slightly increased computational complexity.

**Keywords**: Information fusion, multi-modal data, compressive sensing, detection theory, statistical dependence, copula theory

## I. INTRODUCTION

Multimodal data represents multiple aspects of a phenomenon of interest (PoI) observed using different acquisition methods or different types of sensors [2]. Due to the diversity of information, multimodal data enhances inference performance compared to that with unimodal data. Multimodal data fusion has attracted much attention in different application scenarios such as biometric score fusion [3], [4], multi-media analysis [5], automatic target recognition [6], and footstep detection [7] to name a few. To obtain a unified picture of the PoI to perform a given inference task, multimodal data needs to be fused in an efficient manner. This is a challenging problem in many applications due to complex inter- and intra-modal dependencies and high dimensionality of data.

When the goal is to solve a detection problem in a parametric framework, performing likelihood ratio (LR) based fusion

is challenging since the computation of the joint likelihood functions is difficult in the presence of many unknown parameters and complex inter- and intra- modal dependencies. Different techniques have been proposed to estimate the probability density functions (pdfs) such as histograms, and kernel based methods [3]. In addition to LR based methods, some feature based techniques for multimodal data fusion are discussed in [2]. When the marginal pdfs of data of each modality are available (or can be estimated), which can be disparate due to the heterogeneous nature of multimodal data, copula theory has been used to model inter-modal complex dependencies in [8]–[14]. While there are several copula density functions developed in the literature, finding the best copula function that fits a given set of data is computationally challenging. This is because different copula functions may characterize different types of dependence behaviors among random variables [15], [16]. Finding multivariate copula density functions with more than two modalities is another challenge since most of the existing copula functions are derived considering the bivariate case. Thus, the benefits of the use of copula theory for likelihood ratio based fusion with multimodal dependent data come at a higher computational price. One of the commonly used suboptimal methods is to neglect inter-modal dependence and compute the likelihood functions based on the disparate marginal pdfs of each modality; we call this 'the product approach' in the rest of the paper. The product approach leads to poor performance when the first order statistics of uncompressed data under two hypotheses are not significantly different from each other and/or the inter-modal dependence is strong.

In this paper, we treat the detection problem with heterogeneous dependent data in a compressed domain. In the proposed framework, each node compresses its time samples via low dimensional random projections as proposed in compressive sensing (CS) [17]–[20] and transmits the compressed observation vector to the fusion center. Thus, the communication cost is greatly reduced compared to transmitting all the high dimensional observation vectors to the fusion center. While CS theory has mostly been exploited for sparse signal reconstruction, its potential for solving detection problems has also been investigated in several recent works [21]–[32]. Some of the works, such as [21], [22], [25], [28], [29], [32] focused on constructing decision statistics in the compressed domain exploiting the sparsity prior, some other works [23], [24], [26], [27], [30], [31] considered the detection problem when the signals are not necessarily sparse. When the signal to be detected is known and deterministic, a performance loss is expected in terms of the probabilities of detection and false

alarm when performing likelihood ratio based detection in the compressed domain compared to that with uncompressed data [23]. However, when the signal-to-noise ratio (SNR) is sufficiently large, this loss is not significant and the compressed detector is capable of providing a similar performance as the uncompressed detector. In [31], the authors have extended the known signal detection problem with CS to the multiple sensor case considering Gaussian measurements. While intra-signal (temporal) dependence was considered with Gaussian measurements, inter-sensor (spatial) dependence was ignored in [31]. As mentioned before, with heterogeneous multimodal data, handling inter-modal dependence is one of the key issues in developing efficient fusion strategies. To the best of authors' knowledge, the ability of CS in capturing the dependence properties of uncompressed data to solve detection problems has not been well investigated in the literature.

In this paper, our goal is to exploit the potential of CS to capture dependence structures of high dimensional data focusing on detection problems. We propose a parametric as well as a nonparametric approach for detection with compressed data. In the first approach, we treat the detection problem completely in the compressed domain. With arbitrary disparate marginal pdfs for (temporally independent) uncompressed data of each modality, we employ a Gaussian approximation in the compressed domain and the joint likelihood function of spatially dependent (over modalities) is computed based on multivariate Gaussian pdfs. With this approach, dependence is captured via a compressed version of the covariance matrix of the concatenated (over all the modalities) uncompressed data vector. We show that, under certain conditions, using a small number of compressive measurements (compared to the original signal dimension), better or similar performance can be achieved in the compressed domain compared to performing fusion (i). using the product approach with uncompressed data where inter-modal dependence is completely ignored and (ii). when widely available copula functions are used to model dependence of highly dependent uncompressed data. We further discuss as to how to decide when it is beneficial to perform compressed detection over suboptimal detection with uncompressed dependent data in terms of the Bhattacharya distance measure.

In the second approach, we exploit the potential of CS to capture statistical information of uncompressed data in the compressed domain to compute a test statistic for detection. When uncompressed data is dependent and highly correlated [1] in the presence of the random phenomenon being observed (alternate hypothesis), the covariance matrix of the concatenated data vector (over modalities) is likely to have a different structure compared to the case where the phenomenon is absent (null hypothesis). Thus, a decision statistic can be computed based on the covariance information. Estimation of the covariance matrix of uncompressed data is computationally expensive when the signal dimension is large. Compressive covariance sensing has been discussed in

[33] in which the covariance matrix of uncompressed data is estimated using compressed samples. It is noted that estimation of the complete covariance matrix is not necessary to construct a reliable test statistic for detection. Covariance based test statistics have been proposed for spectrum sensing in [34], [35] without considering any compression. In this paper, depending on the structure of the covariance matrix of uncompressed data, efficient test statistics for detection are computed in the compressed domain, in contrast to the work in [34], [35]. When the difference in second order statistics under two hypotheses is more significant than that with the first order statistics, this approach provides better performance than the first approach with some extra computational complexity. Further, under the same conditions, this approach outperforms the energy detector with compressed as well as with uncompressed data, which is the widely considered nonparametric detector. Moreover, in contrast to the energy detector, the proposed approach is robust, with respect to the threshold setting, against the uncertainties of the signal parameters under the null hypothesis.

The paper is organized as follows. In Section II, background on the detection problem with uncompressed dependent data is discussed. LR based detection with compressed dependent data is considered in Section III. We also discuss when it is beneficial to perform LR based detection with compressed data compared to detection using suboptimal techniques with uncompressed data considering numerical examples. In Section IV, we discuss how to exploit the CS measurement scheme to construct a decision statistic based on the covariance information of uncompressed data. In Section V, CS based detection performance is investigated with real experimental data. Section VI concludes the paper.

*Notation*

The following notation and terminology are used throughout the paper. Scalars are denoted by lower case letters; e.g., $x$. Lower (upper) case boldface letters are used to denote vectors (matrices); e.g., $\mathbf{x}$ ($\mathbf{A}$). Matrix transpose is denoted by $\mathbf{A}^T$. The $n$-th element of the vector $\mathbf{x}_j$ is denoted by both $\mathbf{x}_j[n]$ and $x_{nj}$ while the $(m,n)$-th element of the matrix $\mathbf{A}$ is denoted by $\mathbf{A}[m,n]$. The $j$-th column vector and the $i$-th row vector of $\mathbf{A}$ are denoted by $\mathbf{a}_j$, and $\mathbf{a}^i$, respectively. The trace operator is denoted by $\mathrm{tr}(\cdot)$. The $l_p$ norm of a vector $\mathbf{x}$ is denoted by $||\mathbf{x}||_p$ while the Frobenius norm of a matrix $\mathbf{A}$ is denoted by $||\mathbf{A}||_F$. Calligraphic letters are used to denote sets; e.g., $\mathcal{U}$. We use the notation $|.|$ to denote the absolute value of a scalar, and determinant of a matrix. We use $\mathbf{I}_N$ to denote the identity matrix of dimension $N$ (we avoid using subscript when there is no ambiguity). The vectors of all zeros and ones with an appropriate dimension are denoted by $\mathbf{0}$ and $\mathbf{1}$, respectively. The notation $\mathbf{x} \sim \mathcal{N}(\boldsymbol{\mu}, \boldsymbol{\Sigma})$ denotes that the random vector $\mathbf{x}$ has a multivariate Gaussian pdf with mean vector $\boldsymbol{\mu}$ and covariance matrix $\boldsymbol{\Sigma}$.

## II. Problem Formulation and Background

Let there be $L$ sensor nodes in a network deployed to solve a binary hypothesis testing problem where the two hypotheses

---

[1]Throughout the paper, by 'dependent and correlated', we mean that the data is dependent and has a non-diagonal covariance matrix. When the data is dependent but uncorrelated, i.e., when the dependent data has a diagonal covariance matrix, we use the term 'dependent and uncorrelated'.

are denoted by $\mathcal{H}_1$ and $\mathcal{H}_0$, respectively. The observation vector at each node is denoted by $\mathbf{x}_j \in \mathbb{R}^N$ for $j = 1, \cdots, L$. The goal is to decide as to which hypothesis is true based on $\mathbf{x} = [\mathbf{x}_1^T, \cdots, \mathbf{x}_L^T]^T$.

### A. Likelihood Ratio Based Detection

Consider the detection problem in a parametric framework where the marginal pdf of $\mathbf{x}_j$ is available under both hypotheses. Let $\mathbf{x}_j$ be distributed under $\mathcal{H}_1$ and $\mathcal{H}_0$ as

$$
\begin{aligned}
\mathcal{H}_1 &: \mathbf{x}_j \sim f_1(\mathbf{x}_j) \\
\mathcal{H}_0 &: \mathbf{x}_j \sim f_0(\mathbf{x}_j), j = 1, \cdots, L
\end{aligned}
\tag{1}
$$

respectively, where $f_i(\mathbf{x}_j)$ denotes the joint pdf of $\mathbf{x}_j$ under $\mathcal{H}_i$ for $i = 0, 1$ and $j = 1, \cdots, L$. The optimal test which minimizes the average probability of error based on (1) is the LR test [36] which is given by

$$
\delta = \begin{cases} 1 & \text{if} \quad \frac{f_1(\mathbf{x})}{f_0(\mathbf{x})} > \tau \\ 0 & \text{otherwise} \end{cases}
\tag{2}
$$

where $\tau$ is the threshold. To perform the test in (2), it is required to compute the joint pdfs $f_1(\mathbf{x})$ and $f_0(\mathbf{x})$. The optimality of the LR test is guaranteed only when the underlying joint pdfs are known. When $\mathbf{x}_1, \cdots, \mathbf{x}_L$ are independent under $\mathcal{H}_i$ for $i = 0, 1$, $f_i(\mathbf{x})$ can be written as $f_i(\mathbf{x}) = \prod_{j=1}^L f_i(\mathbf{x}_j)$ for $i = 0, 1$. However, this assumption may not be realistic in practical applications. For example, consider the problem of detection of the presence of a common random phenomenon in a heterogenous signal processing application where there are multiple sensors of different modalities. The data at different nodes may follow disparate marginal pdfs due to the differences in the physics that govern each modality. The presence of the common random phenomenon can change the statistics of the heterogeneous data and make the observations at different modalities dependent [9]. Thus, to detect the presence of the random phenomenon in the LR framework, computation of the joint pdf of data collected at the multiple nodes in the presence of inter-modal dependencies is required.

There are several approaches proposed in the literature to perform LR based detection when the exact pdf of $\mathbf{x}$ is not available. These techniques are commonly categorized as parametric, nonparametric, and semi-parametric approaches.

### B. Copula Theory

In a parametric framework, copulas are used to construct a valid joint distribution describing an arbitrary and possibly nonlinear dependence structure [8]–[15]. According to copula theory, the pdf of $\mathbf{x}$ under $\mathcal{H}_i$ can be written as [15],

$$
f_i(\mathbf{x}) = \prod_{n=1}^N \prod_{l=1}^L f_i(\mathbf{x}_l[n]) c_{ni}(u_{n1}^i, \cdots, u_{nL}^i)
$$

for $i = 0, 1$ where $c_{ni}(\cdot)$ denotes the copula density function, $u_{nl}^i = F(\mathbf{x}_l[n] | \mathcal{H}_i)$ with $F(x | \mathcal{H}_i)$ denoting the marginal cdf

of $x$ under $\mathcal{H}_i$. Then, the log LR (LLR) can be written in the following form:

$$
\begin{aligned}
\Lambda_{\text{LLR}}(\mathbf{x}) &= \log \frac{f_1(\mathbf{x})}{f_0(\mathbf{x})} = \sum_{l=1}^L \sum_{n=1}^N \log \frac{f_1(\mathbf{x}_l[n])}{f_0(\mathbf{x}_l[n])} \\
&+ \sum_{n=1}^N \log \frac{c_{n1}(u_{n1}^1, \cdots, u_{nL}^1 | \phi_{n1})}{c_{n0}(u_{n1}^0, \cdots, u_{nL}^0 | \phi_{n0})}
\end{aligned}
\tag{3}
$$

where $\phi_{n1}$ and $\phi_{n0}$ are copula parameters under $\mathcal{H}_1$ and $\mathcal{H}_0$, respectively, for $n = 1, \cdots, N$. In this case, in general, $N$ copulas where each one is $L$-variate are selected to model dependence. Readers may refer to [8]–[15] to learn more about copula theory as applicable for binary hypothesis testing problems.

One of the fundamental challenges in copula theory is to find the copula density function that will best fit the given data set. Further, most of the copula density functions proposed in the literature consider the bivariate case. In order to model the dependence of multimodal data with more than two modalities, several approaches have been proposed in the literature [13], which are in general computationally complex. Thus, in order to better utilize copula theory for multimodal data fusion, these challenges need to be overcome. In the following, we consider an alternate computationally efficient approach for multimodal data fusion in which dependence among data is modeled in a low dimensional transformed domain obtained via CS. We also discuss the advantages/disadvantages of modeling dependence in the compressed domain via Gaussian approximation over the copula based approach with uncompressed data.

## III. FUSION OF SPATIALLY DEPENDENT DATA IN THE COMPRESSED DOMAIN VIA LIKELIHOOD RATIO TEST

Let $\mathbf{A}_j$ be specified by a set of unique sampling vectors $\{\mathbf{a}_j^m\}_{m=1}^M$ with $M < N$ for $j = 1, \cdots, L$. We assume that the $j$-th node compresses its observations using $\mathbf{A}_j$ so that the compressed measurement vector is given by,

$$
\mathbf{y}_j = \mathbf{A}_j \mathbf{x}_j
\tag{4}
$$

for $j = 1, \cdots, L$ where the $m$-th element of the vector $\mathbf{A}_j \mathbf{x}_j$ is given by $\langle \mathbf{a}_j^m, \mathbf{x}_j \rangle$ for $m = 1, \cdots, M$ where $\langle ., . \rangle$ denotes the inner product. In CS theory, the mapping $\mathbf{A}_j$ is usually selected to be a random matrix. In the rest of the paper, we make the following assumptions: (i) $\mathbf{y}_j$'s are available at the fusion center without an error, (ii) $\mathbf{A}_j$ is an orthoprojector so that $\mathbf{A}_j \mathbf{A}_j^T = \mathbf{I}$, and (iii) the elements of $\mathbf{x}_j$ are independent of each other for given $j$ under both hypotheses while there is (spatial) dependence among $\mathbf{x}_1, \cdots, \mathbf{x}_L$ under $\mathcal{H}_1$ (i.e., there is spatial and temporal independence under $\mathcal{H}_0$ and temporal independence and spatial dependence under $\mathcal{H}_1$).

### A. Likelihood Ratio Based Fusion With Compressed Data

In order to perform LR based fusion based on (4), the computation of the joint pdf of $\{\mathbf{y}_1, \cdots, \mathbf{y}_L\}$ is required. When the marginal pdf of each $\mathbf{x}_j$ is available, the marginal

pdf of each element in $\mathbf{y}_j$ can be computed as in the following. The $m$-th element of $\mathbf{y}_j$, $\mathbf{y}_j[m]$, can be written as,

$$\mathbf{y}_j[m] = \sum_{n=1}^{N} \mathbf{A}_j[m,n]\mathbf{x}_j[n] \tag{5}$$

for $j = 1, \cdots, L$. Having the marginal pdfs of $\mathbf{x}_j[n]$ and using the independence assumption of $\mathbf{x}_j[n]$ for $n = 1, \cdots, N$, the pdf of $z = \mathbf{y}_j[m]$ can be found after computing the characteristic function of $z$. Once the marginal pdfs of the elements in $\mathbf{y}_j$ for $j = 1, \cdots, L$ are found, copula theory can be used in order to find the joint pdf of the compressive measurement vectors $\mathbf{y}_1, \cdots, \mathbf{y}_L$. Letting $u_j = F_j(\mathbf{y}_p[q])$ for $j = M(p-1) + q$ where $p = 1, \cdots, L$, $q = 1, \cdots, M$, the LLR based on copula functions can be expressed as,

$$
\begin{aligned}
&T_{LLR}(\mathbf{y}) \\
&= \sum_{l=1}^{L}\sum_{k=1}^{M} \log \frac{f_1(\mathbf{y}_l[k])}{f_0(\mathbf{y}_l[k])} + \log \frac{c_1(u_1, \cdots, u_{ML}|\phi_1^*)}{c_0(u_1, \cdots, u_{ML}|\phi_0^*)}.
\end{aligned} \tag{6}
$$

The second term on the right hand side of (6) requires one to find copula density functions of $ML$ variables which is computationally very difficult. Since we assume that the elements in $\mathbf{x}_j$ are independent under any given hypothesis, each element in $\mathbf{y}_j$ can be approximated by a Gaussian random variable (via Lindeberg-Feller central limit theorem assuming that the required conditions are satisfied [37], [38]) when $N$ is sufficiently large.

### B. Likelihood Ratio Based Fusion with Compressed Data via Gaussian Approximation

Assume that first and second order statistics of the concatenated data vector $\mathbf{x} = [\mathbf{x}_1^T, \ldots, \mathbf{x}_L^T]^T$ are available. We define additional notation here. Let

$$\boldsymbol{\beta}^i = [\boldsymbol{\beta}_1^{i\,T} \cdots \boldsymbol{\beta}_L^{i\,T}]^T \tag{7}$$

and

$$\mathbf{D}^i = \begin{bmatrix} \mathbf{D}_1^i & \mathbf{D}_{12}^i & \cdots & \mathbf{D}_{1L}^i \\ \mathbf{D}_{21}^i & \mathbf{D}_2^i & \cdots & \mathbf{D}_{2L}^i \\ \cdots & \cdots & \cdots & \cdots \\ \mathbf{D}_{L1}^i & \mathbf{D}_{L2}^i & \cdots & \mathbf{D}_L^i. \end{bmatrix} \tag{8}$$

denote the $NL \times 1$ mean vector and the $NL \times NL$ covariance matrix of $\mathbf{x}$ under $\mathcal{H}_i$ for $i = 0, 1$ where $\boldsymbol{\beta}_j^i = \mathbb{E}\{\mathbf{x}_j|\mathcal{H}_i\}$, $\mathbf{D}_j^i = \mathbb{E}\{(\mathbf{x}_j - \boldsymbol{\beta}_j^i)(\mathbf{x}_j - \boldsymbol{\beta}_j^i)^T|\mathcal{H}_i\}$ and $\mathbf{D}_{jk}^i = \mathbb{E}\{(\mathbf{x}_j - \boldsymbol{\beta}_j^i)(\mathbf{x}_k - \boldsymbol{\beta}_k^i)^T|\mathcal{H}_i\}$ for $j \neq k$ $k = 1, \cdots, L$ and $j = 1, \cdots, L$. With Gaussian approximation, the joint pdf of $\mathbf{y} = [\mathbf{y}_1^T \cdots \mathbf{y}_L^T]^T$ is given by $\mathbf{y}|\mathcal{H}_i \sim \mathcal{N}(\boldsymbol{\mu}^i, \mathbf{C}^i)$ where $\boldsymbol{\mu}^i$ and $\mathbf{C}^i$ are the notations used to define the mean vector and the covariance matrix of $\mathbf{y}$ which are analogous to the definitions in (7) and (8), respectively, with $\boldsymbol{\mu}_j^i = \mathbb{E}\{\mathbf{y}_j|\mathcal{H}_i\}$, $\mathbf{C}_j^i = \mathbb{E}\{(\mathbf{y}_j - \mathbb{E}\{\mathbf{y}_j\})(\mathbf{y}_j - \mathbb{E}\{\mathbf{y}_j\})^T|\mathcal{H}_i\}$, $\mathbf{C}_{jk}^i = \mathbb{E}\{(\mathbf{y}_j - \mathbb{E}\{\mathbf{y}_j\})(\mathbf{y}_k - \mathbb{E}\{\mathbf{y}_k\})^T|\mathcal{H}_i\}$ with $j \neq k$, $k = 1, \cdots, L$ and $j = 1, \cdots, L$ for $i = 0, 1$. We further denote by $\mathbf{D}_x$ ($\mathbf{C}_y$) the covariance matrix of $\mathbf{x}$ ($\mathbf{y}$) where $\mathbf{D}_x = \mathbf{D}^1$ ($\mathbf{C}_y = \mathbf{C}^1$) under $\mathcal{H}_1$ and $\mathbf{D}_x = \mathbf{D}^0$ ($\mathbf{C}_y = \mathbf{C}^0$) under $\mathcal{H}_0$. First and second order statistics of the compressed data are related to that of uncompressed data via

$$\boldsymbol{\mu}_j^i = \mathbf{A}_j\boldsymbol{\beta}_j^i, \mathbf{C}_j^i = \mathbf{A}_j\mathbf{D}_j^i\mathbf{A}_j^T, \text{and } \mathbf{C}_{jk}^i = \mathbf{A}_j\mathbf{D}_{jk}^i\mathbf{A}_k^T$$

for $j, k = 1, \cdots, L$ and $i = 0, 1$. Then, we can write,

$$\boldsymbol{\mu}^i = \mathbf{A}\boldsymbol{\beta}^i \text{ and } \mathbf{C}^i = \mathbf{A}\mathbf{D}^i\mathbf{A}^T$$

where

$$\mathbf{A} = \begin{pmatrix} \mathbf{A}_1 & \mathbf{0} & \cdot & \cdot & \mathbf{0} \\ \mathbf{0} & \mathbf{A}_2 & \cdot & \cdot & \mathbf{0} \\ \cdot & \cdot & \cdot & \cdot & \cdot \\ \mathbf{0} & \mathbf{0} & \cdot & \cdot & \mathbf{A}_L \end{pmatrix} \tag{9}$$

is a $ML \times NL$ matrix. With the assumption that $\mathbf{A}_j\mathbf{A}_j^T = \mathbf{I}_M$ for $j = 1, \cdots, L$, the decision statistic of the LLR based detector is given by [36],

$$
\begin{aligned}
\Lambda_{LLR}(\mathbf{y}) &= \frac{1}{2}\mathbf{y}^T(\mathbf{C}^{0^{-1}} - \mathbf{C}^{1^{-1}})\mathbf{y} \\
&\quad + (\boldsymbol{\mu}^{1^T}\mathbf{C}^{1^{-1}} - \boldsymbol{\mu}^{0^T}\mathbf{C}^{0^{-1}})\mathbf{y} + \tau_0
\end{aligned} \tag{10}
$$

where $\tau_0 = \frac{1}{2}\left(\log\left(\frac{|\mathbf{C}^0|}{|\mathbf{C}^1|}\right) + \boldsymbol{\mu}^{0^T}\mathbf{C}^{0^{-1}}\boldsymbol{\mu}^0 - \boldsymbol{\mu}^{1^T}\mathbf{C}^{1^{-1}}\boldsymbol{\mu}^1\right)$. To compute the threshold so that the probability of false alarm is kept under a desired value, computation of the pdf of $\Lambda_{LLR}$ under $\mathcal{H}_0$ is required. This is in general computationally intractable, but is possible under certain assumptions on $\mathbf{x}$. For example, when $\boldsymbol{\beta}^i = \mathbf{0}$ for $i = 0, 1$ and the elements of $\mathbf{x}$ are identical under $\mathcal{H}_0$ (in addition to independence), we have $\boldsymbol{\mu}^i = \mathbf{0}$ and $\mathbf{C}^0 = \sigma_0^2\mathbf{I}$ where $\sigma_0^2$ denotes the variance of $\mathbf{x}$ under $\mathcal{H}_0$. In this case, the threshold can be computed as considered in [36] (pages 73-75). When such assumptions on $\mathbf{x}$ cannot be made, we propose to compute the threshold via simulations.

*1) Impact of compression on inter-modal dependence:* With the Gaussian approximation after compression, the inter-modal dependence is captured only through the covariance matrix. Higher order dependencies of data are not taken into account in the compressed domain. In particular, $\mathbf{D}_x$ is compressed via $\mathbf{C}_y = \mathbf{A}\mathbf{D}_x\mathbf{A}^T$. To quantify the distortion of $\mathbf{D}_x$ due to compression, one measure is to consider the Frobenius norm of the covariance matrix. We have

$$
\begin{aligned}
||\mathbf{C}_y||_F^2 &= ||\mathbf{A}\mathbf{D}_x\mathbf{A}^T||_F^2 = \mathrm{tr}(\mathbf{A}\mathbf{D}_x^T\mathbf{A}^T\mathbf{A}\mathbf{D}_x\mathbf{A}^T) \\
&= \mathrm{tr}(\mathbf{A}^T\mathbf{A}\mathbf{D}_x^T\mathbf{A}^T\mathbf{A}\mathbf{D}_x) \approx \frac{M^2}{N^2}||\mathbf{D}_x||_F^2
\end{aligned} \tag{11}
$$

where the last approximation is due to $\mathbf{A}^T\mathbf{A} \approx \frac{M}{N}\mathbf{I}$. Thus, the Frobenius norm of the covariance matrix after compression is reduced by a factor of $c_r = \frac{M}{N}$ compared to that with uncompressed data. In other words, the Gaussian approximation in the compressed domain can capture a compressed version of the covariance matrix of uncompressed data. Compared to other approaches with uncompressed data, the product approach does not capture any form of dependence. With respect to copula based approaches, it is not very clear how much dependence can be captured with a given copula function. Since the covariance matrix is not a direct measure of detection performance, in the following subsection we compare the detection performance of different approaches in terms of the average probability of error.

## C. Detection Performance Comparison Between Compressed and Uncompressed Data via Average Probability of Error

In order to quantify the detection performance of different approaches with both uncompressed and compressed data, we consider the Bhattacharya bound (which is a special case of the *Chernoff* bound) which bounds the average probability of error of LR based detectors. We use the notation 'u:product', and 'u:copula-name' for the product approach and the copula based approach with a given copula function stated under 'name', respectively, with uncompressed data. The notation 'c:GA' is used to represent the LR based approach with compressed data using the Gaussian approximation.

The Bhattacharya distance between the two hypotheses with the copula based approach with uncompressed data is given by,

$$
\begin{aligned}
\mathcal{D}_B^{\text{u:copula}}(f_1\|f_0) &= -\log \int f_1^{1/2}(\mathbf{x})f_0^{1/2}(\mathbf{x})d\mathbf{x} \\
&= -\log \mathbb{E}_{f_0}\left\{ \prod_{n=1}^{N}\prod_{l=1}^{L}\left(\frac{f_1^m(\mathbf{x}_l[n])}{f_0^m(\mathbf{x}_l[n])}\right)^{1/2} \right. \\
&\quad \left. c_{n1}^{1/2}(u_{n1}^1,\cdots,u_{nL}^1|\phi_{n1}) \right\}
\end{aligned}
\tag{12}
$$

where $f_i^m$ denotes the marginal pdf under $\mathcal{H}_i$ and we have $f_0(\mathbf{x}) = \prod_{l,n} f_0^m(\mathbf{x}_l[n])$ since we assume $\mathbf{x}_1,\cdots,\mathbf{x}_L$ to be independent of each other under $\mathcal{H}_0$. With the product approach, we have $c_{n1}(\cdot) = 1$ and (12) reduces to,

$$
\begin{aligned}
&\mathcal{D}_B^{\text{u:product}}((f_1\|f_0) \\
&= -\log \mathbb{E}_{f_0}\left\{ \prod_{n=1}^{N}\prod_{l=1}^{L}\left(\frac{f_1^m(\mathbf{x}_l[n])}{f_0^m(\mathbf{x}_l[n])}\right)^{1/2} \right\}.
\end{aligned}
\tag{13}
$$

On the other hand, the Bhattacharya distance between the two hypotheses with compressed data under Gaussian approximation can be computed as [39]

$$
\begin{aligned}
\mathcal{D}_B^{\text{c:GA}}(f_1\|f_0) &= \frac{1}{8}(\boldsymbol{\beta}_1 - \boldsymbol{\beta}_0)^T \Gamma^{\dagger}\boldsymbol{\beta}_1 - \boldsymbol{\beta}_0) \\
&+ \frac{1}{2}\log\{|\Gamma||\mathbf{A}\mathbf{D}^1\mathbf{A}^T|^{-1/2}|\mathbf{A}\mathbf{D}^0\mathbf{A}^T|^{-1/2}\}
\end{aligned}
\tag{14}
$$

where $\Gamma^{\dagger} = \mathbf{A}^T\Gamma^{-1}\mathbf{A}$ and $\Gamma = \frac{1}{2}(\mathbf{A}\mathbf{D}^1\mathbf{A}^T + \mathbf{A}\mathbf{D}^0\mathbf{A}^T)$. Using the Bhattacharya distance, the average probability of error with compressed data, $P_e^c$, is upper bounded by [36],

$$
P_e^c \leq \frac{1}{2}e^{-\mathcal{D}_B^{\text{c:GA}}} \triangleq P_{ub}^{\text{c:GA}}.
$$

Let $\mathcal{D}_B^{\text{u:gvn}}$, and $P_{ub}^{\text{u:gvn}}$ be the Bhattacharya distance, and the upper bound namely the Bhattacharya bound on the probability of error, respectively, with uncompressed data computed using a given suboptimal approach (e.g., product or copula with a given copula function). Then, we have

$$
P_{ub}^{\text{c:GA}} \leq P_{ub}^{\text{u:gvn}} \quad \text{if} \quad \mathcal{D}_B^{\text{c:GA}} \geq \mathcal{D}_B^{\text{u:gvn}}
\tag{15}
$$

where $\mathcal{D}_B^{\text{u:gvn}}$ and $\mathcal{D}_B^{\text{c:GA}}$ are computed as in (12) and (14), respectively. In the case where uncompressed data is dependent and uncorrelated, (15) can be further simplified as stated in Proposition 1.

**Proposition 1.** *Let uncompressed data be dependent and uncorrelated so that $\mathbf{D}^1$ is diagonal. Further, let $\mathbf{D}_j^i = \sigma_{j,i}^2\mathbf{I}$ and $\boldsymbol{\beta}_j^i = \beta_{j,i}\mathbf{1}$ for $i = 0,1$ and $j = 1,\cdots,L$. Then, we have*

$$
P_{ub}^{\text{c:GA}} \leq P_{ub}^{\text{u:gvn}} \quad \text{if} \quad \mathcal{D}_B^{\text{u:gvn}} \leq c_r\rho_B \text{ and}
\tag{16}
$$

*where*

$$
\begin{aligned}
\rho_B &= \frac{N}{2}\left\{ \sum_{j=1}^{L}\log(\sigma_{j,1}^2 + \sigma_{j,0}^2) - \log(\sigma_{j,1}^2\sigma_{j,0}^2) \right. \\
&\quad \left. + \frac{(\beta_{j,1} - \beta_{j,0})^2}{2(\sigma_{j,1}^2 + \sigma_{j,0}^2)} \right\}
\end{aligned}
\tag{17}
$$

*which is determined by the statistics of the uncompressed data and $c_r = \frac{M}{N}$ is the compression ratio.*

*Proof:* The proof follows from the fact that when uncompressed data is uncorrelated under $\mathcal{H}_1$, $\mathcal{D}_B^{c,G}$ in (14) reduces to,

$$
\mathcal{D}_B^{c,G}(f_0\|f_1) = \frac{M}{N}\rho_B
\tag{18}
$$

where $\rho_B$, are as defined in (17). ∎

Thus, whenever $\mathcal{D}_B^{\text{c:GA}} > \mathcal{D}_B^{\text{u:gvn}}$ 'c:GA' performs better than any given suboptimal approach with uncompressed data. Even though $\mathcal{D}_B^{\text{c:GA}} < \mathcal{D}_B^{\text{u:gvn}}$, 'c:GA' can still be promising if the desired performance level in terms of the upper bound on the probability of error is reached. Let $\epsilon_B$ be the desired upper bound on the probability of error. When $\mathcal{D}_B^{\text{c:GA}} \geq -\log(2\epsilon_B)$, 'c:GA' provides the desired performance even if $\mathcal{D}_B^{\text{c:GA}} < \mathcal{D}_B^{\text{u:gvn}}$.

## D. Illustrative Examples

In the following, we consider example scenarios to illustrate the detection performance with 'c:GA' compared to that with uncompressed data using different suboptimal approaches. In the two examples, two types of detection problems are considered. In the first example, we consider a problem of detection of changes in statistics of data collected at heterogeneous sensors. In the second example, detection of a random source by heterogeneous sensors in the presence of noise is considered.

*1) Example 1:* In the first example, we consider $L = 3$ and a common random phenomenon causes a change in the statistics of heterogeneous data at the three sensors. The uncompressed data at the three nodes have the following marginal pdfs: [9]:

$$
\begin{aligned}
x_{n1}|\mathcal{H}_i &\sim \mathcal{N}(0,\sigma_i^2), \; x_{n2}|\mathcal{H}_i \sim \text{Exp}(\lambda_i) \\
&\text{and } x_{n3}|\mathcal{H}_i \sim \text{Beta}(a_i, b_i = 1)
\end{aligned}
\tag{19}
$$

for $i = 0,1$. It is noted that $x \sim \text{Exp}(\lambda)$ denotes that $x$ has an exponential distribution with $f(x) = \lambda e^{-\lambda x}$ for $x \geq 0$ and 0 otherwise, and $x \sim \text{Beta}(a,b)$ denotes that $x$ has a beta distribution with pdf $f(x) = \frac{1}{\mathcal{B}(a,b)}x^{a-1}(1-x)^{b-1}$ and $\mathcal{B}(a,b) = \frac{\Gamma(a)\Gamma(b)}{\Gamma(a+b)}$ is the beta function. The data under $\mathcal{H}_1$ is assumed to be dependent and the following operations are used to generate dependent data. For the data at the second node, we

use $x_{n2} = x_{n1}^2 + w^2$ for $n = 1, \cdots, N$ where $w \sim \mathcal{N}(0, \sigma_1^2)$. Then, we have $x_{n2} \sim \mathrm{Exp}(\lambda_1)$ with $\lambda_1 = \frac{1}{2\sigma_1^2}$. For the third node, the data under $\mathcal{H}_1$ is generated as

$$x_{n3} = \frac{u}{u + x_{n2}}$$

for $n = 1, \cdots, N$ where $u \sim \mathrm{Gamma}(\alpha_1, \beta_1 = 1/\lambda_1)$. Then $x_{n3}|\mathcal{H}_1 \sim \mathrm{Beta}(a_1, b_1 = 1)$ with $a_1 = \alpha_1$. It is noted that $x \sim \mathrm{Gamma}(\alpha, \beta)$ denotes that $x$ has Gamma pdf with $f(x) = \frac{1}{\beta^\alpha \Gamma(\alpha)} x^{\alpha-1} e^{-x/\beta}$ for $x \geq 0$ and $\alpha, \beta > 0$. Under $\mathcal{H}_0$, $x_{n1}$, $x_{n2}$ and $x_{n3}$ are generated independently using the assumed marginal pdfs. In this example, we consider three cases.

*Case I:* In Case I, the data at the first and second sensors are fused. In this case, the covariance matrices of $\mathbf{x} = [\mathbf{x}_1^T \; \mathbf{x}_2^T]^T$ under the two hypotheses, $\mathbf{D}^0$ and $\mathbf{D}^1$, are composed of $\mathbf{D}_1^0 = \sigma_0^2 \mathbf{I}$, $\mathbf{D}_{12}^0 = \mathbf{D}_{21}^0 = \mathbf{0}$, $\mathbf{D}_2^0 = \frac{1}{\lambda_0^2} \mathbf{I}$ under $\mathcal{H}_0$ and $\mathbf{D}_1^1 = \sigma_1^2 \mathbf{I}$, $\mathbf{D}_{12}^1 = \mathbf{D}_{21}^1 = \mathbf{0}$, $\mathbf{D}_2^1 = \frac{1}{\lambda_1^2} \mathbf{I}$ under $\mathcal{H}_1$, respectively. It is worth noting that $\mathbf{D}^1$ is diagonal in this case. Thus, although $\mathbf{x}_1$ are $\mathbf{x}_2$ are spatially dependent under $\mathcal{H}_1$ (by construction), they are uncorrelated, , i. e., higher-order statistics exhibit dependence while the second-order correlation is zero.

*Case II :* For Case II, we consider the fusion of data at the second and third sensors where $\mathbf{x} = [\mathbf{x}_2^T \; \mathbf{x}_3^T]^T$. In this case, we have $\mathbf{D}_2^0 = \frac{1}{\lambda_0^2} \mathbf{I}$, $\mathbf{D}_{23}^0 = \mathbf{D}_{32}^0 = \mathbf{0}$, $\mathbf{D}_3^0 = \frac{a_0}{(a_0+1)^2(a_0+2)} \mathbf{I}$ under $\mathcal{H}_0$ and $\mathbf{D}_2^1 = \frac{1}{\lambda_1^2} \mathbf{I}$, $\mathbf{D}_{23}^1 = \mathbf{D}_{32}^1 = \left( \mathbb{E}_{x_{n1}u}\{\frac{x_{n1}u}{u+x_{n1}}\} - \frac{a_1}{\lambda_1(a_1+1)} \right) \mathbf{I}$, $\mathbf{D}_3^1 = \frac{a_1}{(a_1+1)^2(a_1+2)} \mathbf{I}$ under $\mathcal{H}_1$, respectively. It is noted that $\mathbf{D}^1$ is not diagonal in this case.

*Case III :* In Case III, we consider the fusion of data at all three senors. Also $\mathbf{D}^1$ is not diagonal in this case as well.
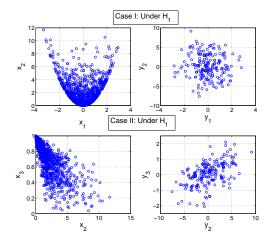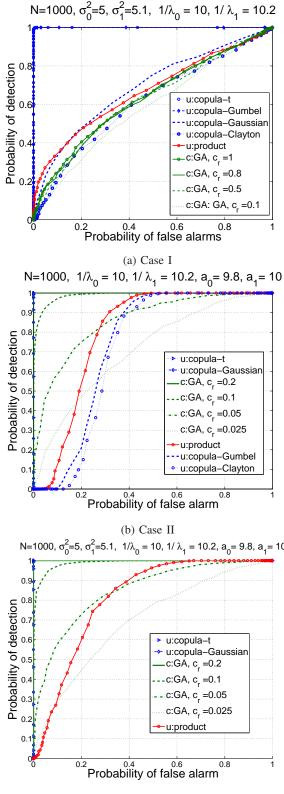


Fig. 1: Scatter plots of uncompressed and compressed data under $\mathcal{H}_1$ in Example 1; $N = 1000$, $M = 200$, $L = 2$

*Scatter plots of uncompressed and compressed data:* First, we illustrate how the dependence structure of data changes going from the uncompressed domain to the compressed domain. In Fig. 1, we show the scatter plots for both compressed and uncompressed data at the two sensors under $\mathcal{H}_1$ for Cases I and II. In Fig. 1, the top and bottom subplots are for Case I and Case II, respectively while the left and right subplots are

for uncompressed and compressed data, respectively. It can be observed that while uncompressed data at the two sensors are strongly dependent, compressed data appears to be weakly dependent. This change of the dependence structure due to compression was addressed in Section III-B1. In this example, the scatter plots of compressed data look more circular (Case I) or elliptical (Case II). In Case 1, even though $x_{n1}$ and $x_{n2}$ for given $n$ are dependent under $\mathcal{H}_1$, they are uncorrelated. This leads to a circular and independent scatter plot for compressed data for Case I.

*Detection With uncompressed data vs. detection with compressed data via Gaussian approximation :* We compare the detection performance of LR based detection with compressed and uncompressed data. The compressed detector with Gaussian approximation, 'c:GA' is compared with the product approach (where dependence is ignored), 'u:product', and the copula based approach, 'u:copula-name', with uncompressed data. For the copula based approach, we consider Gaussian, t, Gumbel and Clayton copula functions as described in [9], [14] for the bivariate case (Cases I and II) and Gaussian and t copula for the tri-variate case (Case III). Fig. 2 shows the performance in terms of the ROC curves for the three cases considered in the example. The parameter values are provided in figure titles. To obtain the ROC curves, $10^3$ Monte Carlo runs were performed throughout unless otherwise specified. With the considered parameter values under the two hypotheses, 'u:product' does not provide perfect detection. We make several important observations here.

- For Case I where uncompressed data at the first two sensors are dependent and uncorrelated ($\mathbf{D}^1$ is diagonal), 'u:product', 'u:copula-t', and 'u:copula-Gumbel' perform much better than 'c:GA' even with $c_r = 1$ as can be seen in Fig. 2(a). In this case, with diagonal $\mathbf{D}^1$, existing higher-order dependence is not taken into account in the compressed domain.

- For Case II where $\mathbf{D}^1$ is not diagonal, as can be seen in Fig. 2(b), 'c:GA' shows a significant performance gain over 'u:product' after $c_r$ exceeds a certain threshold. Fusion with 'u:copula-Gaussian' and 'u:copula-t' leads to perfect detection while the fusion performance with 'c:GA' with fairly small value of $c_r$ is also capable of providing perfect detection for the parameter values considered.

- For Case III, similar results are seen as in Case II when 'c:GA' is compared with 'u:product', 'u:copula-Gaussian', and 'u:copula-t'.

- In Cases II and III, dependence is taken into account via the covariance matrix in the compressed domain as discussed in Section III-B1. Thus, irrespective of the dimensionality reduction, due to the capability to capture a certain amount of dependence in the compressed domain, 'c:GA' is capable of providing a significant performance gain over 'u:product' and comparable performance compared to 'u:copula-Gaussian', and 'u:copula-t'.

- When going from Case II to Case III (i.e., from two sensors to three sensors), 'c:GA' does not show a significant performance improvement for a given value of $c_r$. This is because, only $\mathbf{x}_2$ and $\mathbf{x}_3$ are spatially correlated,

(a) Case I

(b) Case II

(c) Case III

Fig. 2: Performance of dependent data fusion for detection in Example 1: product/copula based approach with uncompressed data vs Gaussian approximation with compressed data: $N = 1000$

and $\mathbf{x}_1$ is uncorrelated with the rest. Thus, the covariance information accounted for in the compressed domain is the same for both cases.

We further illustrate the behavior of the upper bound on the probability of error for Case II. In Fig. 3, we plot the Bhattacharya distance and the upper bound on the probability of error on the left and right subplots, respectively, for the same parameter values as in Fig. 2(b). It is seen that $\mathcal{D}_B^{c:GA}$ is much
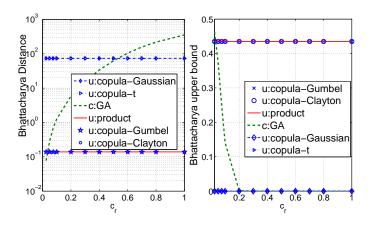


Fig. 3: Bhattacharya distance and the upper on $P_e$ vs $c_r$ with compressed and uncompressed data for Case II in Example 1: $N = 1000$, $1/\lambda_0 = 10$, $1/\lambda_1 = 10.2$, $a_0 = 9.8$, $a_1 = 10$

larger than $\mathcal{D}_B^{u:product}$ for almost all the values of $c_r$. Based on the distance measures shown in the left subplot, it is expected for 'u:copula-Gaussian', and 'u:copula-t' to perform better than CS based detection for smaller values of $c_r$. However, as can be seen in the right subplot in Fig 3, the upper bound on the probability of error with 'c:GA' coincides ($\rightarrow 0$) that with 'u:copula-Gaussian', and 'u:copula-t' when $c_r$ exceeds a certain value. This observation is intuitive since these distance measures are not linearly related to the probability of error. Thus, even though $\mathcal{D}_B^{c:GA} < \mathcal{D}_B^{u:gvn}$ with a given suboptimal approach, compressed detection via 'c:GA' can be promising, as discussed in Subsection III-C.

Since the difference in performance among different approaches varies as the parameter values of the statistics under two hypotheses change, in Fig. 4, we show the ROC curves with another set of parameter values considering Case III for $N = 100$. It can be seen that when the statistics of the data under the two hypotheses are such that 'u:product' does not provide perfect detection, 'c:GA' outperforms 'u:product' when $c_r$ exceeds a certain threshold. Further, as $c_r$ increases, 'c:GA' shows similar performance as with 'u:copula-t' and 'u:copula-Gaussian'. Results in Fig. 4 again verify that the amount of dependence captured in the compressed domain via Gaussian approximation leads to better detection performance than 'u:product' and similar performance as with the copula based approaches.

*2) Example 2:* In the second example, we consider the detection of a signal in the presence of noise with $L = 2$
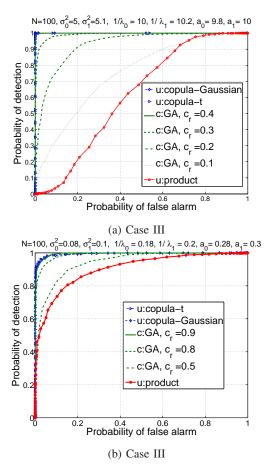
(a) Case III



(b) Case III

Fig. 4: Performance of dependent data fusion for detection in Example 1: product/copula based approach with uncompressed data vs Gaussian approximation with compressed data; $N = 100$

where the signals of interest at the two nodes are (spatially) dependent of each other under $\mathcal{H}_1$. The model for heterogeneous uncompressed sensor data is given by

$$\mathcal{H}_1 : \mathbf{x}_j = \mathbf{s}_j + \mathbf{v}_j$$
$$\mathcal{H}_0 : \mathbf{x}_j = \mathbf{v}_j \qquad (20)$$

for $j = 1, 2$. The noise vector $\mathbf{v}_j$ is assumed to be Gaussian with mean vector $\mathbf{0}$ and covariance matrix $\sigma_v^2\mathbf{I}$. We assume that the $n$-th elements of $\mathbf{s}_1$ and $\mathbf{s}_2$, respectively, are governed by a common random phenomenon so that they are dependent. For illustration purposes, we assume that the dependence model is given by: $s_{n1} = s_n^2 + w_{n1}^2$, $s_{n2} = s_n^2 + u_{n1}^2 + u_{n2}^2$, where the random variables $s_n, w_{n1}, u_{n1}, u_{n2}$ are iid Gaussian with mean zero and variance $\sigma_s^2$. With this model, $s_{n1} \sim \exp(\lambda_1)$ with $\lambda_1 = \frac{1}{2\sigma_s^2}$ and $\frac{s_{n2}}{\sigma_s^2} \sim \mathcal{X}_3^2$ where $x \sim \mathcal{X}_\nu^2$ denotes that $x$ has a chi-squared pdf with degree of freedom $\nu$. Then, it can be shown that the marginal pdfs of $x_{n1}$ and $x_{n2}$ are given by $f_1(x_{n1}|\mathcal{H}_1) = \lambda_1 e^{-\lambda_1 x_{n1}} e^{\frac{\sigma_v^2 \lambda_1^2}{2}} \left(1 - Q\left(\frac{x_{n1}-\sigma_v^2\lambda_1}{\sigma_v}\right)\right)$ where $Q(\cdot)$ denotes the Gaussian $Q$ function and $f_1(x_{n2}|\mathcal{H}_1) = \frac{\sqrt{\sigma_v}}{2\pi\sigma_s^3} e^{\frac{1}{8\sigma_v^2\sigma_s^4}} e^{-\frac{1}{4\sigma_s^2}\left(x_{n2}+\frac{\sigma_v^2}{2\sigma_s^2}\right)^2} G_{-3/2}\left(\frac{\sigma_v^2-2\sigma_s^2 x_{n2}}{2\sigma_s^2\sigma_v}\right)$ where $G_p(z) = \frac{e^{-\frac{z^2}{4}}}{\Gamma(-p)} \int_0^\infty e^{-xz-\frac{x^2}{2}} x^{-p-1} dx$ with $p < 0$. Under

$\mathcal{H}_0$, $x_{n1}$ and $x_{n2}$ have Gaussian pdfs with mean zero and variance $\sigma_v^2$. In this example, we have non-diagonal $\mathbf{D}^1$ with $\mathbf{D}_1^1 = (\sigma_v^2 + \frac{1}{\lambda_1^2})\mathbf{I}$, $\mathbf{D}_{12}^1 = \mathbf{D}_{12}^1 = 2\sigma_s^4\mathbf{I}$ and $\mathbf{D}_2^1 = (\sigma_v^2 + 6\sigma_s^4)\mathbf{I}$.



(a) $N = 100$, $\sigma_v^2 = 2$, $\sigma_s^2 = 0.1$, $1/\lambda_1 = 0.2$



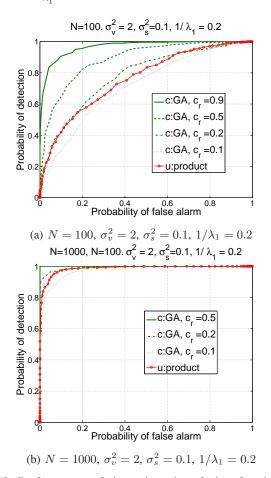(b) $N = 1000$, $\sigma_v^2 = 2$, $\sigma_s^2 = 0.1$, $1/\lambda_1 = 0.2$

Fig. 5: Performance of dependent data fusion for detection in Example 2: Product approach with uncompressed data vs Gaussian approximation with compressed data

In Figs. 5(a) and 5(b), we plot the ROC curves for $N = 100$ and $N = 1000$, respectively. The considered values for $\sigma_v^2$, $\sigma_s^2$ (and $\frac{1}{\lambda_1} = 2\sigma_s^2$) are stated in the figure captions. We compare the performance of 'c:GA' with that of 'u:product'. With the considered parameter values, the performance of 'u:product' with $N = 100$ is not very good. However, 'c:GA' performs significantly better than 'u:product' as $c_r$ increases. With $N = 1000$, 'u:product' shows almost close to prefect detection while similar or better performance is achieved with 'c:GA' with a very small value for $c_r$. As shown in Table II, 'u:product' in this example consumes a significant amount of computational power compared to 'c:GA'. Fig. 5 and Table II verify the applicability of the proposed approach in the presence of spatially dependent and correlated data in terms of both performance and computational complexity.

**Remark 1.** *In Examples 1 and 2, the parameter values are selected such that the mean parameters of uncompressed data under the two hypotheses at a given node are not significantly different from each other. Otherwise, 'u:product' can work well since then the second or higher order statistics are not significant to distinguish between the two hypotheses. In such*

*scenarios, efforts to model dependence do not carry additional benefits to the fusion problem, thus such scenarios are not of interest in this paper.*

**Remark 2.** *Covariance matrices, which measure the degree of linear dependence, partially describe the dependence structure of multivariate data (when the variables are multivariate Gaussian, this description is complete). In particular, when the uncompressed data is non-Gaussian, dependent, and uncorrelated, the covariance information is not capable of characterizing the true dependence. Thus, when such data is compressed via random projections, the dependence information is unaccounted for in the compressed domain while performing 'c:GA'.*

**Remark 3.** *When the uncompressed data is non-Gaussian, dependent and correlated, the covariance information partially characterizes the true dependence. In this case, when the data is compressed via random projections, the dependence information characterized by the covariance matrix (with a certain distortion/change) is partially accounted for in the compressed domain while performing 'c:GA'.*

### E. Computational and Communication Complexity

With 'c:GA', the computational complexity of computing the decision statistic (10) is dominated by the computation of $\mathbf{C}^{1^{-1}}$ (computation of $\mathbf{C}^{0^{-1}}$ is straight forward since $\mathbf{C}^0$ is diagonal due to spatial and temporal independence assumption under $\mathcal{H}_0$). Computation of $\mathbf{C}^{1^{-1}}$ is also straight-forward when the elements of $\mathbf{x}$ are uncorrelated (as considered in Case I in Example 1) since then $\mathbf{C}^1$ becomes diagonal. With spatially correlated uncompressed data, computation of the inverse of a $ML \times ML$ matrix is required. For $L = 2$, $\mathbf{C}^1$ can be partitioned into 4 blocks of each of size $M \times M$, and the matrix inversion Lemma in block form can be exploited. This way, it is necessary to compute the inverse of a $M \times M$ matrix. For $L > 2$, the block inversion Lemma can be still used with nested partitions to compute $\mathbf{C}^{1^{-1}}$. With 'u:product', the likelihood ratio is computed using the given marginal pdfs. For the copula based approaches, computation of the parameters corresponding to a given copula function is required in addition to the computation of the joint marginal pdfs. The parameters that need to be computed for different copula functions considered above are summarized in Table I in [14].

For illustration, we provide in the following, the average run time (in seconds) required to compute the decision statistic for Examples 1 and 2 considered above with different approaches. For Example 1, Cases II and III are considered with $N = 100, 1000$ in Table. I. For Example 2, run times with $N = 100$ and $N = 1000$ are shown in Table II. The run time is computed with MATLAB in a Intel(R) Core(TM) i7-3770 CPU@ 3.40GHzz processor with 12 GB RAM. To estimate the parameters for each copula function, we use the 'copulafit' function and copula density was computed using the function 'copulapdf' in Matlab.

It can be seen that, 'c:GA' with even fairly large $c_r$ ($< \approx 0.5$) consumes less time than all the approaches considered with

TABLE I: Average run time (in seconds) required to compute decision statistics in Example 1

| Approach | $N = 100$ | | $N = 1000$ | |
|---|---|---|---|---|
| | Case II $(L=2)$ | Case III $(L=3)$ | Case II $(L=2)$ | Case III $(L=3)$ |
| 'u:product' | 0.0080 | 0.0281 | 0.0107 | 0.0322 |
| 'u:copula-Gaussian' | 0.0105 | 0.0314 | 0.0138 | 0.0359 |
| 'u:copula-t' | 0.0664 | 0.0948 | 0.2730 | 0.3634 |
| 'c:GA', $c_r = 0.1$ | 1.2239e-04 | 1.2334e-04 | 7.3375e-04 | 0.0016 |
| 'c:GA', $c_r = 0.2$ | 1.4958e-04 | 1.5876e-04 | 0.0016 | 0.0029 |
| 'c:GA', $c_r = 0.5$ | 2.4795e-04 | 2.5894e-04 | 0.0091 | 0.0097 |
| 'c:GA', $c_r = 0.9$ | 3.0501e-04 | 3.5743e-04 | 0.0293 | 0.0294 |

TABLE II: Average run time (in seconds) required to compute decision statistics in Example 2

| Approach | $N = 100$ | $N = 1000$ |
|---|---|---|
| 'u:product' | 0.1425 | 1.4520 |
| 'c:GA', $c_r = 0.1$ | 4.5356e-04 | 0.0092 |
| 'c:GA', $c_r = 0.2$ | 6.8284e-04 | 0.0436 |
| 'c:GA', $c_r = 0.5$ | 0.0027 | 0.4786 |

uncompressed data for both examples. In Example 2 where the marginal pdfs are not readily available to compute the decision statistic for 'u:product', this gap in run times becomes more significant.

In terms of the communication overhead, to perform all the suboptimal approaches considered with uncompressed data, each node is required to transmit its length-$N$ observation vector to the fusion center. On the other hand, with 'c:GA', each node is required to transmit only a length-$M$ ($M < N$) vector. Thus, the communication overhead, in terms of the total number of messages to be transmitted by each node, is reduced by a factor of $c_r = \frac{M}{N}$ with 'c:GA' compared to all the approaches with uncompressed data.

In summary, from Examples 1 and 2, we can conclude the following:

- The computational complexity of 'c:GA' with small $c_r$ is significantly less than that with the other approaches with uncompressed data.
- The communication overhead of 'c:GA' is reduced by a factor $c_r$ compared to all the other approaches with uncompressed data.
- 'c:GA' performs significantly better than 'u:product' and shows similar/comparable performance as that with the copula based approach when the covariance matrix of uncompressed data under $\mathcal{H}_1$ is non-diagonal given that the mean parameters of data under the two hypotheses are not significantly different from each other.
- With dependent but uncorrelated uncompressed data, 'c:GA' can still be advantageous in terms of the computational/communication complexity at the expense of a small loss of performance compared to 'u:product' and quite significant performance loss compared to the copula based approaches.

## IV. DETECTION WITH COMPRESSED DEPENDENT DATA BASED ON SECOND ORDER STATISTICS OF UNCOMPRESSED DATA

In Section III, the detection problem was solved in the compressed domain assuming that the marginal pdfs and the first and second order statistics of the uncompressed data under each hypothesis are known (or can be accurately estimated). However, these assumptions may be too restrictive in practical settings. In the following, we consider a nonparametric approach where the goal is to compute a decision statistic for detection based on the statistics of uncompressed data where such statistics are estimated from compressed measurements. Consider that each node (modality) has access to a stream of data $\mathbf{x}_j(t)$ for $t = 1, \cdots, T$. Further let $\mathbf{x}(t) = [\mathbf{x}_1(t)^T, \cdots, \mathbf{x}_L(t)^T]^T$ and redefine $\mathbf{D}_x$ to be the covariance matrix of $\mathbf{x}(t)$. We consider a decision statistic of the form

$$\Lambda_{\text{cov}} = f(\mathbf{D}_x).$$

Under $\mathcal{H}_0$, $\mathbf{D}_x$ is diagonal with the assumption that the data is independent across time and space. Under $\mathcal{H}_1$, $\mathbf{D}_x$ can have off-diagonal elements in the presence of spatially correlated multimodal data. Since the covariance matrix has different structures under the two hypotheses, a decision statistic based on uncompressed covariance matrix can be computed. There are several covariance based decision statistics computed in [34], [35]. Covariance absolute value (CAV) detection is considered in [34], [35]. With CAV, the decision statistic becomes

$$\Lambda_{\text{cov}} = \frac{\sum_i \sum_j |\mathbf{D}_x[i,j]|}{\sum_i |\mathbf{D}_x[i,i]|}. \tag{21}$$

With this statistic, when there are off-diagonal elements in the covariance matrix, we have $\Lambda_{\text{cov}} > 1$ while $\Lambda_{\text{cov}} = 1$ when the off diagonal elements are zeros. The goal is to get an approximation to $\Lambda_{\text{cov}}$ based on compressed data $\mathbf{y}(t) = \mathbf{A}\mathbf{x}(t)$ for $t = 1, \cdots, T$ where $\mathbf{A}$ is as defined in (9).

The covariance matrix of $\mathbf{y}(t)$, $\mathbf{C}_y$, can be expressed as

$$\mathbf{C}_y = \mathbf{A}\mathbf{D}_x\mathbf{A}^T.$$

Note that, $\sum_i \mathbf{D}_x[i,i] = \text{tr}(\mathbf{D}_x)$. We have

$$\text{tr}(\mathbf{C}_y) = \text{tr}(\mathbf{A}\mathbf{D}_x\mathbf{A}^T) = \text{tr}(\mathbf{A}^T\mathbf{A}\mathbf{D}_x).$$

When $\mathbf{A}_j$ is selected as an orthoprojector for $j = 1, \cdots, L$, we may approximate $\mathbf{A}^T\mathbf{A} \approx \frac{M}{N}\mathbf{I}$. Then, we have

$$\text{tr}(\mathbf{C}_y) \approx \frac{M}{N}\text{tr}(\mathbf{D}_x),$$

and, thus, $\text{tr}(\mathbf{D}_x) = \frac{N}{M}\text{tr}(\mathbf{C}_y)$. Here we approximate $\mathbf{C}_y$ by the sample covariance matrix computed as

$$\tilde{\mathbf{C}}_y = \frac{1}{T}\sum_{t=1}^{T}[\mathbf{y}(t) - \mathbb{E}(\mathbf{y}(t))][\mathbf{y}(t) - \mathbb{E}(\mathbf{y}(t))]^T. \tag{22}$$

Then, the decision statistic (21) reduces to

$$\Lambda_{\text{cov}} = \frac{\eta + 2\sum_{i=1}^{NL-1}\sum_{j=i+1}^{NL}|\mathbf{D}_x[i,j]|}{\eta} \tag{23}$$

where $\eta = \frac{N}{M}\text{tr}(\tilde{\mathbf{C}}_y)$.

The goal is to estimate the off-diagonal elements of $\mathbf{D}_x$ based on $\tilde{\mathbf{C}}_y$. It is noted that estimation of the complete covariance matrix, $\mathbf{D}_x$, is not necessary to construct $\Lambda_{\text{cov}}$ in (23). In the case where only spatial samples are dependent and the time samples of each modality are independent, the covariance matrix has only a $2(L-1)$ diagonals (in addition to the main diagonal) with nonzero elements. In the following, we describe a procedure to compute $\Lambda_{\text{cov}}$ in (23) based on $\tilde{\mathbf{C}}_y$ when there is spatial dependence of data so that $\mathbf{D}_x$ has a known structure. Note that we may write $\tilde{\mathbf{C}}_y$ as

$$\tilde{\mathbf{C}}_y = \sum_{i,j}\mathbf{D}_x[i,j]\mathbf{a}_i\mathbf{a}_j^T. \tag{24}$$

Let $\mathcal{U}$ be a set consisting of $(i,j)$ pairs corresponding to the desired off-diagonal elements in the upper (or lower) triangle of $\mathbf{D}_x$. The $m$-th pair in $\mathcal{U}$ is denoted by, $(\mathcal{U}(m,1), \mathcal{U}(m,2))$ and $\tilde{N} = |\mathcal{U}|$.

**Proposition 2.** *Let $\mathbf{d}_U$ be the vector containing elements $\mathbf{D}_x[i,j]$ for $(i,j) \in \mathcal{U}$. The least squares solution of $\mathbf{d}_U$ is given by*

$$\hat{\mathbf{d}}_U = \mathbf{B}^{-1}\mathbf{b} \tag{25}$$

*where $\mathbf{B}$ is a $\tilde{N} \times \tilde{N}$ matrix whose $(m,r)$-th element is given by*

$$\mathbf{B}[m,r] = \mathbf{a}_{\mathcal{U}(r,2)}^T\mathbf{a}_{\mathcal{U}(m,2)}\mathbf{a}_{\mathcal{U}(m,1)}^T\mathbf{a}_{\mathcal{U}(r,1)} \tag{26}$$

*and $\mathbf{b}$ is a $\tilde{N} \times 1$ vector with*

$$\mathbf{b} = [\mathbf{a}_{\mathcal{U}(1,2)}^T\tilde{\mathbf{C}}_y^T\mathbf{a}_{\mathcal{U}(1,1)}, \cdots, \mathbf{a}_{\mathcal{U}(\tilde{N},2)}^T\tilde{\mathbf{C}}_y^T\mathbf{a}_{\mathcal{U}(\tilde{N},1)}]^T. \tag{27}$$

*Proof:* Let $\mathbf{R} = \tilde{\mathbf{C}}_y - \sum_{(i,j)\in\mathcal{U}}\mathbf{D}_x[i,j](\mathbf{a}_i\mathbf{a}_j^T + \mathbf{a}_j\mathbf{a}_i^T) = \tilde{\mathbf{C}}_y - \sum_{m=1}^{\tilde{N}}\mathbf{d}_U[m]\tilde{\mathbf{A}}_m$ where $\tilde{\mathbf{A}}_m = \mathbf{a}_{\mathcal{U}(m,1)}\mathbf{a}_{\mathcal{U}(m,2)}^T + \mathbf{a}_{\mathcal{U}(m,2)}\mathbf{a}_{\mathcal{U}(m,1)}^T$. The LS solution of $\mathbf{d}_U$ is found by solving

$$\hat{\mathbf{d}}_U = \arg\min_{\mathbf{d}_U}||\mathbf{R}||_F^2 = \arg\min_{\mathbf{d}_U}\text{tr}(\mathbf{R}\mathbf{R}^T). \tag{28}$$

We can express $\text{tr}(\mathbf{R}\mathbf{R}^T)$ as,

$$\text{tr}(\mathbf{R}\mathbf{R}^T) = \text{tr}(\tilde{\mathbf{C}}_y\tilde{\mathbf{C}}_y^T) - 2\tilde{\mathbf{b}}^T\mathbf{d}_U + \mathbf{d}_U^T\tilde{\mathbf{B}}\mathbf{d}_U \tag{29}$$

where $\tilde{\mathbf{b}}[m] = \text{tr}(\tilde{\mathbf{C}}_y\tilde{\mathbf{A}}_m^T)$ for $m = 1, \cdots, \tilde{N}$ and $\tilde{\mathbf{B}}[m,r] = \text{tr}(\tilde{\mathbf{A}}_m\tilde{\mathbf{A}}_m^T)$ for $m, r = 1, \cdots, \tilde{N}$. Taking the derivative of (29) with respect to $\mathbf{d}_U$, $\hat{\mathbf{d}}_U$ is found as

$$\hat{\mathbf{d}}_U = \tilde{\mathbf{B}}^{-1}\tilde{\mathbf{b}}. \tag{30}$$

It can be easily shown that $\tilde{\mathbf{B}} = 2\mathbf{B}$ and $\tilde{\mathbf{b}} = 2\mathbf{b}$ where $\mathbf{B}$ and $\mathbf{b}$ are as defined in (26) and (27), respectively, resulting in (25) which completes the proof. ∎

Then, $\Lambda_{\text{cov}}$ in (23) reduces to

$$\Lambda_{\text{cov}} = \frac{\eta + 2||\hat{\mathbf{d}}_U||_1}{\eta}. \tag{31}$$

## A. Illustrative Example

To illustrate the detection performance with the test statistic $\Lambda_{\text{cov}}$ in (31), we consider Example 1 given in Section III-D with Case II, in which the goal is to detect the change of the statistical parameters due to a common random phenomenon. Uncompressed data is generated based on the considered marginal pdfs under the two hypotheses and the dependence model under $\mathcal{H}_1$ the as considered in Case II in Example 1. Detection using (31) is performed assuming that the second order statistics of uncompressed data are not known under any hypothesis and estimating them with compressed measurements. For this case, there are only two nonzero off diagonals of $\mathbf{D}_x$ in which the values are the same (say $d_U$). To compute $\Lambda_{\text{cov}}$, estimation of only $d_U$ is required which is given by $\hat{d}_U = \frac{\mathbf{b}^T \mathbf{1}}{\mathbf{1}^T \mathbf{B} \mathbf{1}}$ where $\mathbf{B}$ and $\mathbf{b}$ are as defined in (26) and (27), respectively.



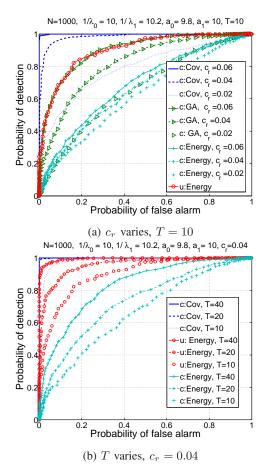(a) $c_r$ varies, $T = 10$



(b) $T$ varies, $c_r = 0.04$

Fig. 6: Detection performance with the test statistic (31); $N = 1000$
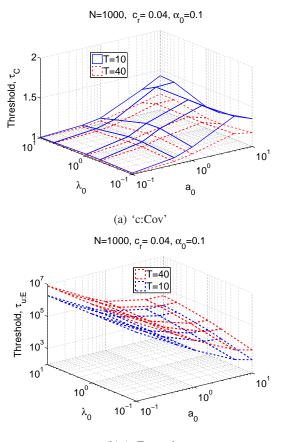
In Fig. 6, we plot ROC curves with the test statistic (31) for different values for $c_r$ and $T$ where $T$, as defined earlier, is the number of sample vectors available for each modality. The detector with the test statistic (31) is denoted as 'c:Cov'. The parameters used to generate data under the two hypotheses are the same as were used in Fig. 2 (b). ROC curves are generated using 1000 Monte Carlo runs. In Fig. 6 (a), the performance of 'c:Cov' is shown for different values of $c_r$ keeping $T = 10$. We compare the results obtained using the energy detector

with compressed as well as uncompressed data, denoted by 'c:Energy', and 'u:Energy', respectively, which is a widely used nonparametric detector. The test statistic of 'u:Energy' and 'c:Energy' is given by $\Lambda_{\text{u:Energy}} = \sum_{t=1}^{T} \|\mathbf{x}(t)\|_2^2$, and $\Lambda_{\text{c:Energy}} = \sum_{t=1}^{T} \|\mathbf{y}(t)\|_2^2$, respectively. Further the detection performance with Gaussian approximation, 'c:GA', is also shown which assumes that the statistics of uncompressed data are known. With the parameter values considered, for given $c_r$ and $T$, it is seen from Fig. 6 (a) that 'c:Cov' significantly outperforms 'c:Energy' and 'c:Cov'. Compared to 'u:Energy', 'c:Cov' outperforms 'u:Energy' after $c_r$ exceeds a certain value (which is very small). In Fig. 6 (b), the detection performance is shown as $T$ varies for $c_r = 0.04$ so that $M = 40$. As can be seen in Fig. 6 (b), detection performance improves as $T$ increases for all the detectors. For 'c:Cov', the estimate of $\hat{d}_U$ becomes more accurate as $T$ increases. However, the value of $T$ that is capable of providing almost perfect detection with 'c:Cov' is not very large compared to $M$. As can be seen in Fig. 6 (b), almost perfect detection is achieved when $T = 20$ for the parameter values considered which is less than $M$. Further, 'c:Cov' outperforms 'u:Energy' and 'c:Energy' for all the values of $T$ considered while the performance gain achieved by 'c:Cov' is significant compared to 'c:Energy'.

Next, we illustrate the robustness of 'c:Cov'. A CAV based test statistic as in (21) has been used to detect a signal in the presence of Gaussian noise in [34], [35] without any compression. It has been shown that the threshold required to keep the probability of false alarm, $P_f$, under a desired value, $\alpha_0$, is independent of the noise power making the CAV based detector more robust than the energy detector against the uncertainties of the noise power. With the CAV based test statistic computed in this paper based on the compressed data as in (31), the computation of the threshold, $\tau_C$, in closed-form so that $P_f \leq \alpha_0$ is computationally intractable. In the above example, uncompressed data under $\mathcal{H}_0$ is non-Gaussian and the marginal pdfs of data at the two sensors are parameterized by $\lambda_0$ and $a_0$, respectively. In Fig. 7, we plot the threshold vs $\lambda_0$ and $a_0$ to ensure $P_f \leq \alpha_0$ keeping $N$ are $T$ are fixed. With 'u:Energy', $\Lambda_{\text{u:Energy}}|\mathcal{H}_0$ can be approximated by a Gaussian random variable with mean $\mu_{u,E}$ and variance $\sigma_{u,E}^2$ as $NT$ is sufficiently large where $\mu_{u,E} = NT\left(\frac{2}{\lambda_0^2} + \frac{a_0}{a_0+2}\right)$ and $\sigma_{u,E}^2 = NT\left(\frac{20}{\lambda_0^2} + \frac{4a_0}{(a_0+4)(a_0+2)^2}\right)$. Then, the threshold, $\tau_{u,E}$, so that $P_f \leq \alpha_0$ can be obtained as $\tau_{u,E} = NT\left(\frac{2}{\lambda_0^2} + \frac{a_0}{a_0+2}\right) + Q^{-1}(\alpha_0)\sqrt{NT\left(\frac{20}{\lambda_0^2} + \frac{4a_0}{(a_0+4)(a_0+2)^2}\right)}$ where $Q^{-1}(\cdot)$ denotes the inverse Gaussian $Q$ function. Similarly with 'c:Energy', the threshold $\tau_{c,E}$ can be found as $\tau_{c,E} = MT\left(\frac{2}{\lambda_0^2} + \frac{a_0}{a_0+2}\right) + Q^{-1}(\alpha_0)\sqrt{MT\left(\frac{20}{\lambda_0^2} + \frac{4a_0}{(a_0+4)(a_0+2)^2}\right)}$.

In Fig. 7, the threshold required to keep $P_f \leq \alpha_0$ with 'c:Cov'' and 'u:Energy' vs $a_0$ and $\lambda_0$ is shown for given $N$ and $T$. It can be observed that the variation of $\tau_C$ with respect to $a_0$ and $\lambda_0$ is fairly small (negligible). However, $\tau_{u:E}$ varies significantly as $a_0$ and $\lambda_0$ vary (similar observations are

seen for $\tau_{c:E}$ while the figures are not included for brevity). Thus, in addition to the performance gain achieved over 'u:Energy' (and 'c:Energy'), 'c:Cov' is more robust against the uncertainties of the signal parameters under $\mathcal{H}_0$ than the energy detector.



(a) 'c:Cov'



(b) 'u:Energy'

Fig. 7: Threshold of 'c:Cov' and 'u:Energy' vs $a_0$ and $\lambda_0$

### B. Computational Complexity

For $\Lambda_{\text{cov}}$, the computation of $\mathbf{B}^{-1}$ and $\mathbf{b}$ as in (26) and (27), respectively is required in addition to computing the sample covariance matrix $\tilde{\mathbf{C}}_y$. Computation of $\Lambda_{\text{u:Energy}}$ and $\Lambda_{\text{c:Energy}}$ is straight forward from $\mathbf{x}(t)$ and $\mathbf{y}(t) = \mathbf{A}\mathbf{x}(t)$, respectively, for $t = 1, \cdots, L$. The run times required to compute the decision statistics for the four approaches considered in Fig. 6(a) are listed in Table III when the input is given as $\mathbf{x}(t)$ for $t = 1, \cdots, L$. The statistic of 'c:GA' is independent of $T$ since we assume perfect knowledge of the covariance matrix of uncompressed data for the Gaussian approximation based approach. It is noted that, the decision statistic was computed over $10^3$ trials to get the average run time. From Table III, it can be observed that a relatively large run time is required for 'c:Cov' compared to the other approaches. This is the price to pay for the performance gain achieved as depicted in Fig. 6 (a) and the robustness in threshold setting against the signal parameters under $\mathcal{H}_0$ as depicted in Fig. 7. Further, in 'c:Cov', the run time does not significantly increase when $T$ increases

(going from $T = 10$ to $T = 40$) although this increase in $T$ can improve the performance as can be seen in Fig. 6 (b).
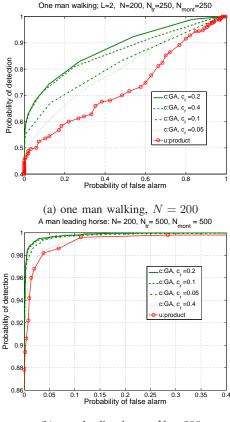
TABLE III: Average run time (in seconds) required to compute decision statistics for 'c:Cov', 'c:GA', 'c:Energy' and 'u:Energy' for Case II in Example 2

| Approach | $N = 1000$ $T = 10$ | $N = 1000$ $T = 40$ |
|---|---|---|
| 'u:Energy' | 6.1529e-04 | 0.0027 |
| 'c:Energy' $c_r = 0.02$ | 3.4280e-04 | 7.7378e-04 |
| 'c:Energy' $c_r = 0.04$ | 4.5460e-04 | 0.0011 |
| 'c:Energy' $c_r = 0.06$ | 5.3973e-04 | 0.0014 |
| 'c:GA' $c_r = 0.02$ | 4.0746e-04 | 4.0746e-04 |
| 'c:GA' $c_r = 0.04$ | 4.9580e-04 | 4.9580e-04 |
| 'c:GA' $c_r = 0.06$ | 5.5683e-04 | 5.5683e-04 |
| 'c:Cov' $c_r = 0.02$ | 0.0137 | 0.0148 |
| 'c:Cov' $c_r = 0.04$ | 0.0163 | 0.0178 |
| 'c:Cov' $c_r = 0.06$ | 0.0258 | 0.0277 |

## V. EXPERIMENTAL RESULTS WITH REAL DATA

To further validate the detection performance with multimodal data in the compressed domain with the proposed approaches, in this section, we consider real experimental data. We use the footstep data, made available by the US Army Research Laboratory (ARL), collected at the US southwest border. The dataset consists of raw observations from several acoustic, seismic and PIR sensors that were deployed in an outdoor space to record human and animal activity that is typical in perimeter and border surveillance scenarios. The participants in the data collection exercise walked/ran along a predetermined path with sensors laid out along either side of the path.

In the following experiments, we consider two cases; detection of one man walking and a man leading a horse based on data at two sensors (one acoustic and one seismic). Each seismic/acoustic time series contains a leading $60s$ of background data. For the detection problem, we use this as $\mathcal{H}_0$ data. The data are sampled at $10kHz$, and are mean centered and oscillatory in nature. The time series data at each sensor was split into non-overlapping frames of size $N$. Further, $N_{tr}$ frames were used for training under each hypothesis and $N_{mont}$ frames were used for test.

In Fig. 8, we show the performance when detection is performed with 'c:GA' (it is noted that we show the detection performance only with the Gaussian approximation due to the limited number of samples to implement the covariance based approach). The mean and the covariance matrices of compressed data under each hypotheses are estimated using the training data. The values used for $N$, $N_{tr}$ and $N_{mont}$ for the two cases are shown in figure titles. We further plot the detection performance with 'u:product'. To obtain the marginal pdfs of uncompressed data under $\mathcal{H}_1$, a kernel based density estimate is computed using the training data with the Gaussian kernel. Under $\mathcal{H}_0$, the data is assumed to be iid Gaussian where the mean and the variance were estimated using the training data.

(a) one man walking, $N = 200$



(b) man leading horse; $N = 200$

Fig. 8: Detection performance with compressed and uncompressed data; $L = 2$ (one seismic and one acoustic sensor)

For both cases, it is observed that 'c:GA' with a small compression ratio, (e.g., $c_r = 0.05$), outperforms detection with 'u:product'. Another observation is that, when $c_r$ increases beyond a certain threshold, the performance does not monotonically improve (e.g., performance with $c_r = 0.2$ is better than that with $c_r = 0.4$ in Fig. 8). This is because, when $c_r$ (thus $M$) increases, more training samples are needed to estimate $\mathbf{C}^0$ and $\mathbf{C}^1$ accurately as required in (10). When the amount of training data available is limited, the estimates of $\mathbf{C}^0$ and $\mathbf{C}^1$ become less accurate as $M$ increases leading to degraded detection performance. However, with the available (limited) number of samples, detection with 'c:GA' provides better performance with small $c_r$ values than detection using the product approach with uncompressed data.

## VI. CONCLUSION

Optimal decision fusion with high dimensional multimodal dependent data is a challenging problem. In this paper, we explored the potential of CS in capturing the dependence structures of spatially dependent data to develop efficient decision statistics for detection in the compressed domain. In addition to the inherent benefits of CS in terms of low computational and communication overhead compared to processing and transmitting high dimensional data, we showed that the performance of CS based detection with dependent data using LR can be better than or similar to several suboptimal detection

techniques with uncompressed data under certain conditions. We discussed conditions under which modeling dependence in the compressed domain using Gaussian approximation is more efficient and effective than modeling dependence with uncompressed data which is computationally expensive most of the time. We further discussed a nonparametric approach for detection where a decision statistic is computed based on the covariance matrix of uncompressed data and the statistic is estimated in the compressed domain. This approach can provide better performance when the non-Gaussian uncompressed data is highly correlated with an additional computational cost compared to that is required for the Gaussian approximation based approach. Further, the proposed compressed covariance based detector is more robust than the widely considered nonparametric detector; the energy detector.

## REFERENCES

[1] T. Wimalajeewa and P. K. Varshney, "Detection with multimodal dependent data using low dimensional random projections," in *42nd Int. Conf. Acoustics, Speech, and Signal Processing (ICASSP)*, New Orleans, LA, Mar. 2017.

[2] D. Lahat, T. Adali, and C. Jutten, "Multimodal data fusion: An overview of methods, challenges, and prospects," *Proc. IEEE*, vol. 103, no. 9, pp. 1449–1477, 2015.

[3] K. Nandakumar, Y. Chen, S. C. Dass, and A. K. Jain, "Likelihood ratio based biometric score fusion," *IEEE Trans. Pattern Anal. Mach. Intell.*, vol. 30, pp. 342–347, Feb. 2008.

[4] E. T. Adall, "Special section on multimodal biomedical imaging: Algorithms and applications," *IEEE Trans. Multimedia*, vol. 15, no. 5, Aug. 2013.

[5] P. K. Atrey, M. A. Hossain, A. E. Saddik, and M. S. Kankanhalli, "Multimodal fusion for multimedia analysis: a survey," *Multimedia Systems*, vol. 16, no. 6, pp. 345–379, Apr. 2010.

[6] H. Zhang, N. M. Nasrabadi, Y. Zhang, and T. S. Huang, "Multi-view automatic target recognition using joint sparse representation," *IEEE Trans. Aerosp. Electron. Syst.*, vol. 48, pp. 2481–2497, 2012.

[7] X. Jin, S. G. A. Ray, and T. Damarla, "Multimodal sensor fusion for personnel detection," in *Proceedings of 14th International Conference on Information Fusion*, Chicago, IL, July 2011.

[8] G. Mercier, G. Moser, and S. Serpico, "Conditional copula for change detection on heterogeneous SAR data," in *Proc. IEEE Int. Geosci. Remote Sens. Symp. (IGARSS)*, July 2007, pp. 2394–2397.

[9] S. G. Iyengar, P. K. Varshney, and T. Damarla, "A parametric copula-based framework for hypothesis testing using heterogeneous data," *IEEE Trans. Signal Process.*, vol. 59, no. 5, pp. 2308–2318, May 2011.

[10] A. Sundaresan and P. K. Varshney, "Location estimation of a random signal source based on correlated sensor observations," *IEEE Trans. Signal Process.*, vol. 59, no. 2, pp. 787–799, Feb. 2011.

[11] A. Sundaresan, P. K. Varshney, and N. S. V. Rao, "Copula-based fusion of correlated decisions," *IEEE Trans. Aerosp. Electron. Syst.*, vol. 47, no. 1, p. 454=471, Jan. 2011.

[12] S. G. Iyengar, P. K. Varshney, and T. Damarla, "Biometric authentication: A copula-based approach," in *Multibiometrics for Human Identification*, B. Bhanu and V. Govindaraju, Eds. Cambridge University Press, 2011, pp. 95–119.

[13] A. Subramanian, A. Sundaresan, and P. K. Varshney, "Fusion for the detection of dependent signals using multivariate copulas," in *14th International Conference on Information Fusion*, Chicago, Illinois, USA, 2011, pp. 740–747.

[14] H. He and P. K. Varshney, "Fusing censored dependent data for distributed detection," *IEEE Trans. Signal Process.*, vol. 63, no. 16, pp. 4385–4395, Aug. 2015.

[15] R. Nelsen, *An Introduction to Copulas*, 2nd ed. New York: Springer, 2006.

[16] D. Mari and S. Kotz, *Correlation and Dependence*. Imperial College Press, 2001.

[17] E. Candès, J. Romberg, and T. Tao, "Robust uncertainty principles: exact signal reconstruction from highly incomplete frequency information," *IEEE Trans. Inf. Theory*, vol. 52, no. 2, pp. 489 – 509, Feb. 2006.

[18] E. Candès and T. Tao, "Near-optimal signal recovery from random projections: Universal encoding strategies?" *IEEE Trans. Inf. Theory*, vol. 52, no. 12, pp. 5406 – 5425, Dec. 2006.

[19] D. Donoho, "Compressed sensing," *IEEE Trans. Inf. Theory*, vol. 52, no. 4, pp. 1289–1306, Apr. 2006.

[20] Y. C. Eldar and G. Kutyniok, *Compressed Sensing: Theory and Applications*. Cambridge University Press, 2012.

[21] M. F. Duarte, M. A. Davenport, M. B. Wakin, and R. G. Baraniuk, "Sparse signal detection from incoherent projections," in *Proc. Acoust., Speech, Signal Processing (ICASSP)*, May 2006.

[22] J. Haupt and R. Nowak, "Compressive sampling for signal detection," in *Proc. Acoust., Speech, Signal Processing (ICASSP)*, vol. 3, Honolulu, Hawaii, Apr. 2007, pp. III–1509 – III–1512.

[23] M. A. Davenport, P. T. Boufounos, M. B. Wakin, and R. Baraniuk, "Signal processing with compressive measurements," *IEEE J. Sel. Topics Signal Process.*, vol. 4, no. 2, pp. 445 – 460, Apr. 2010.

[24] T. Wimalajeewa, H. Chen, and P. K. Varshney, "Performance analysis of stochastic signal detection with compressive measurements," in $44^{\text{th}}$ *Annual Asilomar Conf. on Signals, Systems and Computers*, Nov. 2010, pp. 913–817.

[25] G. Li, H. Zhang, T. Wimalajeewa, and P. K. Varshney, "On the detection of sparse signals with sensor networks based on Subspace Pursuit," in *IEEE Global Conference on Signal and Information Processing (GlobalSIP)*, Atlanta, GA, Dec. 2014, pp. 438–442.

[26] B. Kailkhura, T. Wimalajeewa, L. Shen, and P. K. Varshney, "Distributed compressive detection with perfect secrecy," in *2nd Int. Workshop on Compressive Sensing in Cyber-Physical Systems (CSCPS'14)*, Oct. 2014.

[27] B. Kailkhura, T. Wimalajeewa, and P. K. Varshney, "On physical layer secrecy of collaborative compressive detection," in $48^{\text{th}}$ *Annual Asilomar Conf. on Signals, Systems and Computers*, 2014.

[28] B. S. M. R. Rao, S. Chatterjee, and B. Ottersten, "Detection of sparse random signals using compressive measurements," in *Proc. Acoust., Speech, Signal Processing (ICASSP)*, 2012, pp. 3257–3260.

[29] J. Cao and Z. Lin, "Bayesian signal detection with compressed measurements," *Information Sciences*, pp. 241–253, 2014.

[30] B. Kailkhura, S. Liu, T. Wimalajeewa, and P. K. Varshney, "Measurement matrix design for compressed detection with secrecy guarantees," *IEEE Wireless Commun. Lett.*, vol. 5, no. 4, pp. 420–423, Aug. 2016.

[31] B. Kailkhura, T. Wimalajeewa, and P. K. Varshney, "Collaborative compressive detection with physical layer secrecy constraints," *IEEE Trans. Signal Process.*, vol. 65, no. 4, pp. 1013–1025, Feb. 2017.

[32] T. Wimalajeewa and P. K. Varshney, "Sparse signal detection with compressive measurements via partial support set estimation," *IEEE Trans. on Signal and Inf. Process. over Netw.*, vol. 3, no. 1, Mar. 2017.

[33] D. Romero, D. Ariananda, Z. Tian, and G. Leus, "Compressive covariance sensing: Structure-based compressive sensing beyond sparsity," *IEEE Signal Process. Mag.*, vol. 33, no. 1, pp. 78–93, Jan. 2016.

[34] Y. Zeng and Y.-C. Liang, "Covariance based signal detections for cognitive radio," in *IEEE Int. Symposium on New Frontiers in Dynamic Spectrum Access Networks*, Dublin, Ireland, Apr. 2007, pp. 202–207.

[35] ——, "Spectrum-sensing algorithms for cognitive radio based on statistical covariances," *IEEE Trans. Veh. Technol.*, vol. 58, no. 4, pp. 1804–1815, May 2009.

[36] H. V. Poor, *An Introduction to Signal Detection and Estimation*. New York: Springer-Verlag, 1994.

[37] H. Cramer, *Mathematical Methods of Statistics*. Princeton, New Jersey: Princeton University Press, 1946.

[38] T. Wimalajeewa, H. Chen, and P. K. Varshney, "Performance limits of compressive sensing-based signal classification," *IEEE Trans. on Signal Process.*, vol. 60, no. 6, pp. 2758–2770, June 2012.

[39] K. Abou-Moustafa and F. Ferrie, "A note on metric properties for some divergence measures: The gaussian case," *J. Mach. Learn. Res.*, vol. 25, pp. 1–15, Nov. 2012.